Tcchnical Paper

Journal of the Society of
Naval Architects of Korea
Vol. 27, No. 2, June 1990
大 韓 造 船 學 會 誌
第27卷 第2號 1990年 6月

Velocities Induced by Stator Arrays in a Class of Shear Flows

by

E.D. Park*

전단 유동중에 놓인 스테이터에 의한 유기속도

박 의 동*

Abstract

The interaction of the flows induced by stator blades with a ship-like wake is discussed to obtain the flow components of each with and without radial shear.

The flow induced by stator blades is modeled by lifting line theory and the shear is taken to be provided by the radial gradient of the peripheral mean axial flow approximated by a logarithmic function of radius for a class of vessels. And the theory is based on the linearized Euler equations in the absence of viscosity.

The results show that shear effects are relatively large at inner radii and the distribution of blade pitch angles is most effective in reducing non-uniformity.

국문요약

선미 반류중에 놓인 스테이터에 의하여 유기되는 속도성분을 전단 유동일 경우와 전단 유동이 아닌 경우에 대하여 다루었다.

스테이터 날개에 의한 속도 성분 계산에는 양력선 이론이 사용되었으며 전단성분은 반류성분이 반경의 로그 함수로 표시 가능한 선형의 평균 반류 분포에 대한 반경 방향의 기울기로 나타내었다.

그리고 기본이론은 점성이 없는 경우의 오일러 방정식에 기초를 두었다. 계산결과, 전단 유동의 영향은 허브에 가까울수록 커졌으며 반류의 불균일을 감소시키는데는 스테이터 날개에 피치를 분포하는 것이 가장 효과적이었다.

1. Introduction

This study is directed principally at the determination of the spatial harmonics of the velocity components downstream of an array of atator blades which are immersed in a spatially varying flow as produced in the region of the propeller by the hull of a ship moving on a straight course at constant speed. Such incident hull flows have a peripheral mean axial component which varies radially and is assumed to be independent of axial position. The presence of this shear, $-\frac{dU}{dr}$, gives rise to additional velocity components because of the coupling

발표 : 대한조선학회 '89년도 춘계연구발표회('89. 4. 23)
접수일자 : 1989년 5월 2일, 재접수일자 : 1990년 2월 13일
* 정회원, 진해기계창

between itself and the velocity field induced by the stators.

One of earliest studies of the distortion of inviscid, incompressible onset flows with vorticity by the flow about a body was that of Young and Maas[1] in 1936, who calculated the effect of the dividing stream line about a pitot tube due to a lateral shear in the incident stream. In 1944 Von Kármán and Tsien[2] analyzed the flow about a wing in a stream with transverse and vertical shears. While they gave no numerical results, their analysis indicated that the coupling of the shear and the transverse perturbation velocity grows without bound far downstream. It was their opinion that nonetheless the results would be useful in the vicinity of the wing. In the 1950's Lighthill[3][4][5][6] dealt with fundamental aspects of flows generated by singularities intracting with generally weak shears. He also noted downstream divergences.

In regard to propeller hydrodynamics there was no attention to shear intractions until 1976 when Breslin[7] proposed a study of actuator disc-shear flow intraction in response to difficulties experienced by the U.S. Navy in prediction of submarine powering characteristics from self-propelled model tests. As a result, several analyses were made by Goodman[8], Goodman and Valentine[9]. Comparisons of Goodman's theory with water tunnel measurements were made by Goodman and Breslin[10] which displayed very good agreement when account was taken of the non-linear induction of the moderately loaded propellers. A significant advance was made by Huang and Groves[11] using a finite difference method for the flow on a body of revolution with and without propeller induction.

The present theory is based on the Euler's equation of motion for an incompressible, inviscid fluid in which only the radial shear is retained as characterizing the dominant vorticity in the hull-generated non-uniform flow. A solution is obtained for a class of shear flows satisfying $\left(\frac{d^2}{dr^2}-\frac{1}{r}\frac{d}{dr}\right)\frac{1}{U(r)}=0$. This class of hull wake flow has been found to yield quite reasonable agreement with measurements made on models. The stator blades are represented by thin body theory in regard to their thickness effects and by lifting line theory for their loading induced flow.

Attention is focused on the spatial harmonics of the axial and tangential components immediately downstream of the stator array with variations of angular position of stator arrays and blade pitch angles because one of the purposes of the stator is to ameliorate the non-uniformity of the flow at the propeller plane.

2. Induced Velocities due to Lift

2.1 Formulation of the problem

We consider inviscid, incompressible and steady incident main flow whose axial component varies with radius, i.e., $U=U(r)$, and in which u, v and w are the axial, tangential and radial components induced by a stator array immersed in this flow. These components are assumed to be small relative to U.

In cylinderical coordinates(x, r, γ) as shown in Figure 1, the linearized Euler equations are,

$$\text{axial;}\quad -U(r)\frac{\partial u}{\partial x}-\frac{dU}{dr}w+\frac{1}{\rho}\frac{\partial p}{\partial x}=0 \qquad (2\text{-}1)$$

$$\text{tangential;}\quad -U(r)\frac{\partial v}{\partial x}+\frac{1}{\varphi r}\frac{\partial p}{\partial \gamma}=-\frac{F(s,\theta)}{\rho}\frac{\delta(x)\delta(r-s)\delta(\gamma-\theta)}{r} \qquad (2\text{-}2)$$

$$\text{radial;}\quad -U(r)\frac{\partial w}{\partial x}+\frac{1}{\rho}\frac{\partial p}{\partial r}=0 \qquad (2\text{-}3)$$

where $F(s,\theta)$ is the lift force per unit length generated by a stator blade element in tangential direction.

The continuity equation is,

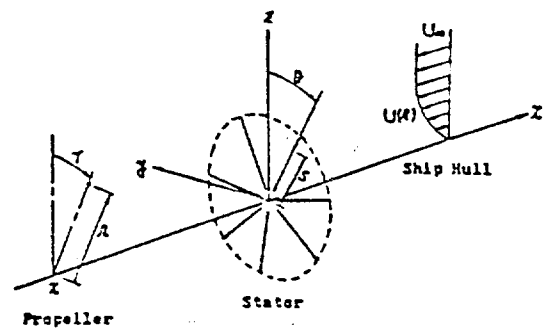

Fig. 1 Cylinderical coordinates at stator and propellar planes

$$\frac{\partial u}{\partial x}+\frac{w}{r}+\frac{\partial w}{\partial r}+\frac{1}{r}\frac{\partial v}{\partial \gamma}=0 \qquad (2\text{-}4)$$

Operating on (2-1), (2-2) and (2-3) by, $-\frac{\partial}{\partial x}$, $\frac{1}{r}\frac{\partial}{\partial \gamma}$, $\frac{\partial}{\partial r}$, respectively and adding in $\frac{1}{r}$ times (2-3), and using (2-4) yields,

$$\nabla^2 p-\frac{2}{U}(\nabla U\cdot\nabla p)=-\frac{F(s,\theta)}{r^2}\delta(x)\delta(r-s)\delta'(\gamma-\theta)$$

By introducing a new function $\psi(x, r, \gamma; s, \theta)$, where $\psi=V(r)P$, and $V(r)=\frac{1}{U(r)}$,

$$\nabla^2\psi-\left(\frac{\nabla^2 V}{V}\right)=-\frac{V}{r^2}F(s,\theta)\delta(x)\delta(r-s)\delta'(\gamma-\theta) \qquad (2\text{-}5)$$

Equation (2-5) can be converted to an integral equation by using the general form of the solution of a Poisson equation for an unbounded domain.[12]

$$\psi=-\frac{1}{4\pi}\int_{-\infty}^{\infty}dx'\int_0^{\infty}r'dr'\int_0^{2\pi}d\gamma'\frac{\nabla^2 V(r')}{V(r')}\frac{\psi(x',r',\gamma')}{R}+\frac{1}{4\pi}\int_{-\infty}^{\infty}dx'\int_0^{\infty}\frac{r'dr'}{(r')^2}\int_0^{2\pi}d\gamma' V(r')F(s,\theta)\frac{\delta(x')\delta(r'-s)\delta(\gamma'-\theta)}{R} \qquad (2\text{-}6)$$

where $R=\sqrt{(x-x')^2+r^2+(r')^2-2rr'\cos(\gamma-\gamma')}$

From experimental wake data for a class of bodies, as shown in Figure 2. we see that the distribution of dimensionless nominal wake is well approximated in the disc region by

$$\frac{U(r)}{U_\infty}=\frac{1}{1.30-1.19\ \ln\ (r/R_s)} \quad r<\delta^*$$
$$=1 \quad \delta^*<r \qquad (2\text{-}7)$$

where R_s ; radius of stator blades, and

$\delta^*\cong 1.29R_s$; boundary layer thickness

For this class of wake distributions given in (2-7),

$\nabla^2 V=0$ except at $r=\delta^*$

$$w=-\frac{1}{4\pi\rho}\int_h^b ds\frac{F(s,\theta)}{U(s)}\frac{(r^2-s^2)\sin(\gamma-\theta)}{[r^2+s^2-2rs\cos(\gamma-\theta)]^2}\left\{1-\frac{x}{\sqrt{x^2+r^2+s^2-2rs\cos(\gamma-\theta)}}\right\}$$
$$+\frac{1}{4\pi\rho}\int_h^b ds\frac{F(s,\theta)}{U(s)}\frac{r-s\cos(\gamma-\theta)}{r^2+s^2-2rs\cos(\gamma-\theta)}\frac{xr\sin(\gamma-\theta)}{[x^2+r^2+s^2-2rs\cos(\gamma-\theta)]^{3/2}} \qquad (2\text{-}9)$$
$$+\frac{U'(r)}{4\pi\rho U(r)}\int_h^b ds\frac{F(s,\theta)}{U(s)}\frac{r\sin(\gamma-\theta)}{r^2+s^2-2rs\cos(\gamma-\theta)}\left\{1-\frac{x}{\sqrt{x^2+r^2+s^2-2rs\cos(\gamma-\theta)}}\right\}$$

2.2.2. Axial Component

Integrating (2-1) over x, from x to ∞, and using the boundary condition and the expressions for w and P, we obtain

$$u=-\frac{1}{4\pi\rho}\int_h^b ds\frac{F(s,\theta)}{U(s)}\frac{r\sin(\gamma-\theta)}{[x^2+r^2+s^2-2rs\cos(\gamma-\theta)]^{3/2}}$$
$$+ds\frac{U'}{4\pi\rho U}\int_h^b ds\frac{F(s,\theta)}{U(s)}\frac{(r^2-s^2)\sin(\gamma-\theta)}{[x^2+r^2+s^2-2rs\cos(\gamma-\theta)]^2}\{x-\sqrt{x^2+r^2+s^2-2rs\cos(\gamma-\theta)}\}$$

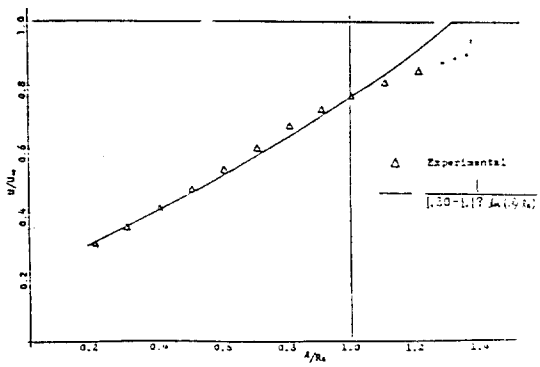

Fig. 2 Experimental wake data and its approximation

Hence (2-6) is changed to,

$$\psi=\frac{1}{4\pi}\int_{-\infty}^{\infty}dx'\int_0^{\infty}\frac{r'dr'}{(r')^2}\int_0^{2\pi}d\gamma' V(r')F(s,\theta)\frac{\delta(x')\delta(r'-s)\delta'(\gamma'-\theta)}{R}$$

Since lift force acts along the entire blade, from hub to tip, the total perturbation pressure becomes,

$$P=-\frac{U(r)}{4\pi}\int_h^b\frac{ds}{s}\frac{F(s,\theta)}{U(s)}\frac{\partial}{\partial\gamma'}\left(\frac{1}{R}\right)_{\gamma'=\theta}$$

or,

$$P(x,r,\gamma;s,\theta)=\frac{U(r)}{4\pi}\int_h^b\frac{ds}{s}\frac{F(s,\theta)}{U(s)}\frac{\partial}{\partial\gamma}\left(\frac{1}{R}\right)$$

Induced velccities can be calculated by using the pressure equation, together with boundary conditions far upstream. These conditions are,

$$u=v=w=0$$
$$P=0 \qquad \text{at } x\to\infty \qquad (2\text{-}8)$$

2.2 Induced velocities

2.2.1 Radial Component

Integrating (2-3) over x, from x to ∞, and using the pressure equation and the boundary condition, we have

$$+\frac{U'}{4\pi\rho U}\int_h^b ds\,\frac{F(s,\theta)}{U(s)}\,\frac{r-s\cos(\gamma-\theta)}{r^2+s^2-2rs\cos(\gamma-\theta)}\,\frac{r\sin(\gamma-\theta)}{\sqrt{x^2+r^2+s^2-2rs\cos(\gamma-\theta)}} \tag{2-10}$$

$$-\frac{(U')^2}{4\pi\rho U^2}\int_h^b ds\,\frac{F(s,\theta)}{U(s)}\,\frac{r\sin(\gamma-\theta)}{r^2+s^2-2rs\cos(\gamma-\theta)}\left\{x-\sqrt{x^2+r^2+s^2-2rs\cos(\gamma-\theta)}\right\}$$

2.2.3. Tangential Component

Integrating (2-2) over x, from x to ∞, and using the pressure equation, the boundary condition and the properties of the Dirac delta function,

$$v=-\frac{F(r,\theta)}{2\pi\rho rU(r)}+\frac{1}{4\pi\rho}\int_h^b\frac{ds}{s}\,\frac{F(s,\theta)}{U(s)}\,\frac{xr}{[x^2+r^2+s^2-2rs\cos(\gamma-\theta)]^{3/2}}$$

$$-\frac{1}{4\pi\rho}\int_h^b\frac{ds}{s}\,\frac{F(s,\theta)}{U(s)}\,\frac{r-s\cos(\gamma-\theta)}{r^2+s^2-2rs\cos(\gamma-\theta)}\left\{1-\frac{x}{\sqrt{x^2+r^2+s^2-2rs\cos(\gamma-\theta)}}\right\} \tag{2-11}$$

$$-\frac{r}{4\pi\rho}\int_h^b ds\,\frac{\partial}{\partial s}\left\{\frac{F(s,\theta)}{sU(s)}\right\}\frac{r-s\cos(\gamma-\theta)}{r^2+s^2-2rs\cos(\gamma-\theta)}\left\{1-\frac{x}{\sqrt{x^2+r^2+s^2-2rs\cos(\gamma-\theta)}}\right\}$$

2.3. Lift force

A stator blade of aspect ratio ≥ 4 can be represented by a lifting line with the distribution of circulation along the line passing through the quarter chord from the leading edge, The lift force density is, by the Kutta-Joukowsky theorem,

$$F(s,\theta)=-\rho U(s)\Gamma(s,\theta) \tag{2-12}$$

This lift force can be expressed in terms of the local lift coefficient, i.e.,

$$F(s,\theta)=-\frac{1}{2}\rho cU^2(s)C_L \tag{2-13}$$

Here we are concerned with the lift arising from the non-uniformity of the hull wake, Prandtle-type strip theory expresses C_L as a function of the nominal angle of attack and the induced angle of attack[13], or,

$$C_L=2\pi(\alpha_w-\alpha_i) \tag{2-14}$$

where

$$\alpha_w=\frac{v_w}{U},\ \text{and}\ \alpha_i=\frac{v_i}{U}$$

Equating (2-12) and (2-13), and using (2-14), we obtain

$$\Gamma(s,\theta)=\pi c(s)\{v_w(s,\theta)-v_i(s,\theta)\} \tag{2-15}$$

$$F(s,\theta)=-\pi\rho c(s)U(s)\{v_w(s,\theta)-v_i(s,\theta)\} \tag{2-16}$$

And $\Gamma(s,\theta)=0$

$F(s,\theta)=0$ at hub and tip.

3. Induced Velocities due to Thickness

3.1. Formulation of the problem

The linearized Euler equations in cylinderical coodinates without external forces are,

$$\text{axial};\ -U(r)\frac{\partial u}{\partial x}-\frac{dU}{dr}w+\frac{1}{\rho}\frac{\partial p}{\partial x}=0 \tag{3-1}$$

$$\text{tangential};\ -U(r)\frac{\partial v}{\partial x}+\frac{1}{\rho r}\frac{\partial p}{\partial\gamma}=0 \tag{3-2}$$

$$\text{radial};\ -U(r)\frac{\partial w}{\partial x}+\frac{1}{\rho}\frac{\partial p}{\partial r}=0 \tag{3-3}$$

The distribution of thickness for thin blades can be represented by distributions of scurces and sinks along the center plane of the blade. If there exist sources in a flow field the continuity equation is expressed as,

$$\frac{\partial u}{\partial x}+\frac{w}{r}+\frac{\partial w}{\partial r}+\frac{1}{r}\frac{\partial v}{\partial\gamma}=\frac{m(x_0,s)}{r}\,\delta(x-x_0)\,\delta(r-s)\,\delta(\gamma-\theta) \tag{3-4}$$

where $m(x_0,s)$ is source strength at given x_0 and s.

According to the same procedure given at part 2.1, we can obtain pressure equation.

$$P(x,r,\gamma)=-\frac{\rho U(r)}{4\pi}\int_h^b ds\int_{-c/2}^{c/2}dx_0\,m(x_0,s)\,\frac{\partial}{\partial x}\left(\frac{1}{R}\right) \tag{3-5}$$

where $m(x_0,s)=-2U(s)\dfrac{\partial\tau(x_0,s)}{\partial x_0}$

and τ is half thickness of blade section.

3.2. Induced velocites

By the similiar procedure given at part 2, we obtain,

$$w=\frac{1}{2\pi}\int_h^b ds\,U(S)\int_{-c/2}^{c/2}dx_0\left\{\frac{\partial\tau(x_0)}{\partial x_0}\,\frac{\partial}{\partial r}\left(\frac{1}{R}\right)-\frac{U'(r)}{U(r)}\tau(x_0)\,\frac{\partial}{\partial x_0}\left(\frac{1}{R}\right)\right\} \tag{3-6}$$

$$u=-\frac{1}{4\pi}\int_h^b ds\int_{-c/2}^{c/2}dx_0\,m(x_0,s)\,\frac{\partial}{\partial x}\left(\frac{1}{R}\right)-\frac{U'}{2\pi U}\int_h^b U(s)ds\int_{-c/2}^{c/2}dx_0\,\tau(x_0)\,\frac{\partial}{\partial r}\left(\frac{1}{R}\right)-\frac{(U')^2}{2\pi U^2}\int_h^b U(s)ds\int_{-c/2}^{c/2}dx_0\,\frac{\tau(x_0)}{R} \tag{3-7}$$

$$v=-\frac{1}{4\pi r}\int_h^b ds\int_{-c/2}^{c/2} dx_0\, m(x_0,s)\frac{\partial}{\partial r}\left(\frac{1}{R}\right) \quad (3\text{-}8)$$

3.3. Thickness distribution

Blade thickness is symmetrically disposed about the design camber surface. Here we take the thickness as symmetrical ogival section, i.e., composed of two circular arcs. For these sections, the ogive can be very closely approximated by a parabola,[14] as shown in Figure 3, whose equation is

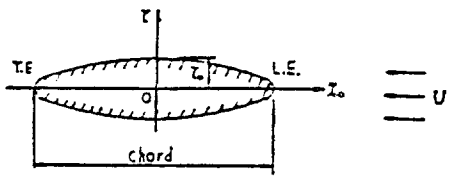

Fig. 3 Thickness distribution of blade section

$$\tau(x_0)=-\frac{4\tau_0}{c^2}\left(x_0-\frac{c}{2}\right)\left(x_0+\frac{c}{2}\right) \quad (3\text{-}9)$$

where τ_0 is the maximum semi-thickness at $x=0$, and

$$\frac{d\tau}{dx_0}=-\frac{8\tau_0}{c^2}x_0 \quad (3\text{-}10)$$

4. Effects of the Number of Blades

To achieve the total induced velocities for a Z-bladed stater, we may replace θ by θ_n and sum over n from $n=1$ to $n=Z$, i.e.,

$$u(x,r,\gamma;Z)=\sum_{n=1}^{Z}u(x,r,\gamma;Z=1,\theta\to\theta_n) \quad (4\text{-}1)$$

For an equally spaced stator array, we may replace θ by $\theta+(2\pi\ n/Z)$ and sum over $n=0$ (key blade) to $n=Z-1$, i.e.,

$$u(x,r,\gamma;Z)=\sum_{n=0}^{Z-1}u(x,r,\gamma;Z=1,\ \theta\to\theta+2\pi\ n/Z) \quad (4\text{-}2)$$

5. Effects of Pitch Angles

If we impose a gecmentric angle of attack along the blade, the lift coefficient in (2-3) is changed to

$$C_L=2\pi(\alpha_p+\alpha_w-\alpha_i) \quad (5\text{-}1)$$

where α_p is pitch angle, and (2-14) is changed to

$$\Gamma(s,\theta)=\pi c(s)\{U(s)\alpha_p+v_w(s,\theta)-v_i(s,\theta)\} \quad (5\text{-}2)$$

$$F(s,\theta)=-\pi\rho c(s)U(s)\{U(s)\alpha_p+v_w(s,\theta)-v_i(s,\theta)\}$$

6. Harmonic Analysis

On the single-screw ship we assume that flow symmetry exists between the port and starboard side. Thus in Fourier analysis we consider even functions for the axial velocity component and odd functions for tangential velocity component when the key blade is located at 12 o'clock, otherwise we consider both even and odd functions.

Let $u,v,w=f(\gamma)$ at given x and r, then

$$f(\gamma)=A_c+\sum_{n=1}^{\infty}A_n\cos(n\gamma-\phi) \quad (6\text{-}1)$$

where A_0 is mean value

A_n is n-th harmonic amplitude

ϕ is phase angle

And

$$A_0=\frac{1}{2\pi}\int_0^{2\pi}f(\gamma)d\gamma \quad (6\text{-}2)$$

$$A_n=\frac{1}{\pi}\int_0^{2\pi}f(\gamma)\cos(n\gamma-\phi)d\gamma \quad (6\text{-}3)$$

7. Numerical Calculation and Results

Numerical calculations are carried out for three nominal axial velocities; six angular positions of the key blade of equally spaced stator arrays; and five variations of blade pitch angles as shown in Tables 1, 2, 3 and 4.

Table 1 Conditions for nominal axial velocity

Case I	Non-uniform nominal axial velocity Shear is Included
Case II	Non-uniform nominal axial velocity Shear is neglected
Case III	Uniform nominal axial velocity

Table 2 Angular positions of the key blade(radian)

Case 1	0	12 O'clock position
Case 2	$2\pi/42$	Clockwise
Case 3	$2\pi/42\times2$	
Case 4	$2\pi/42\times3$	
Case 5	$2\pi/42\times4$	
Case 6	$2\pi/42\times5$	

Table 3 Conditions for blade pitch angles

Case A	Zero pitch angle
Case B	$\alpha_p=0.5v_\omega/U$
Case C	$\alpha_p=1.0v_\omega/U$
Case D	$\alpha_p=1.5v_\omega/U$
Case E	$\alpha_p=2.0v_\omega/U$

All length scales are non-dimensionalized by stator radius R_s, and velocity scales are non-dimensionalized by ship speed U. Simpson's rule is used in spanwise and chordwise integrals.

Axial and tangential induced velocities and their harmonic components with the variation of angular positions and pitch angles are given in Figures 4 to 10.

Table 4 Principal characteristics and field points

x : $=-0.5R_s$	axial position of a propeller
h : $0.2R_s$	stator hub radius
r : 9 points	$0.2R_s$, $0.3R_s$, $0.4R_s$, $\cdots$, $1.0R_s$
γ : 42 points	equally divided
z : 7	equally spaced
c : $0.1R_s$	constant
τ_0 : $c/8$	maximum semi-thickness

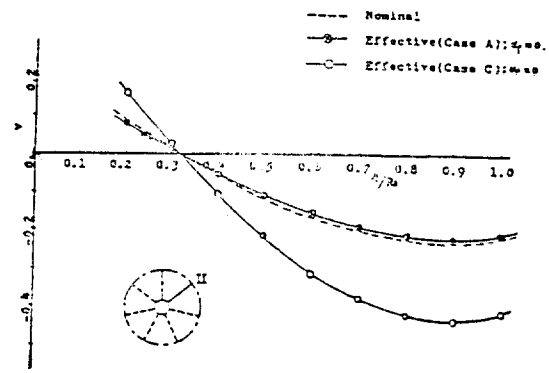

Fig. 4 Nominal and effective tangential velocities, Blade No. II. Case I-1

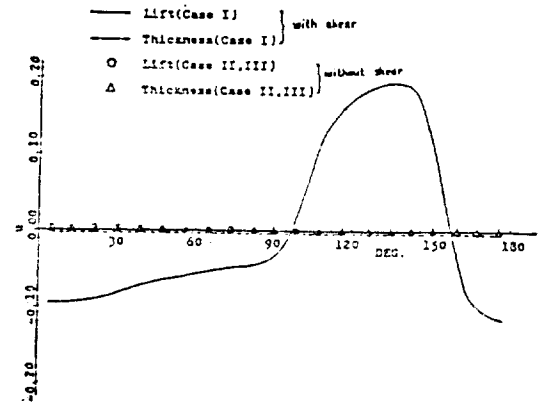

Fig. 5 Axial induced velocities due to lift forces and thickness, $0.2R_s$, Case 1-A ($\alpha_p=0$)

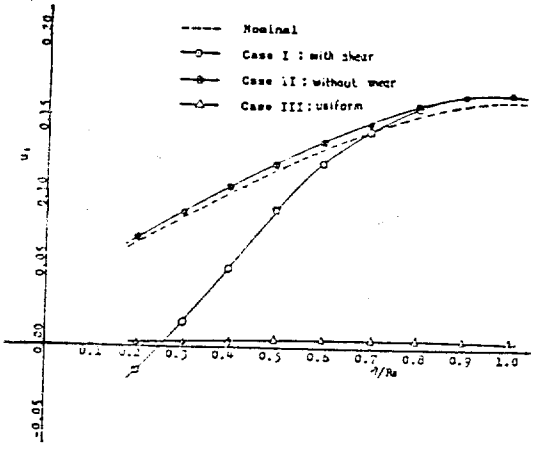

Fig. 6 Harmonic amplitude of axial velocity at propeller plane, $n=1$. Case 1-A ($\alpha_p=0$)

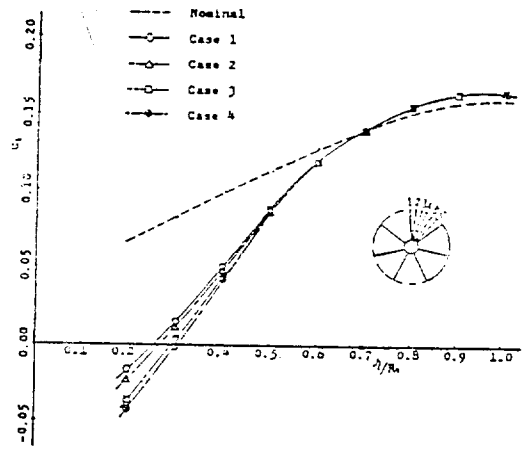

Fig. 7 Harmonic amplitude of axial velocity at propeller plane, $n=1$. Case I-A (with shear, $\alpha_p=0$)

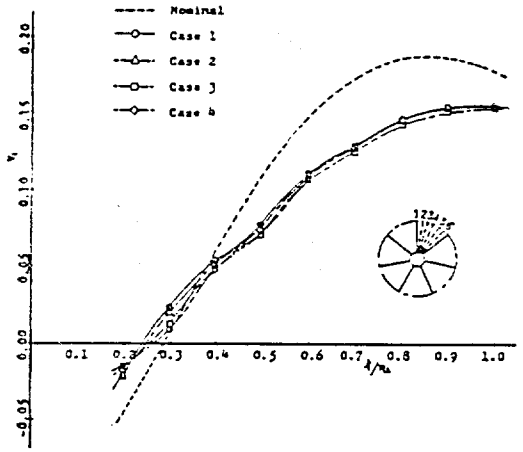

Fig. 8 Harmonic amplitude of tangential velocity at propeller plane, $n=1$, Case A

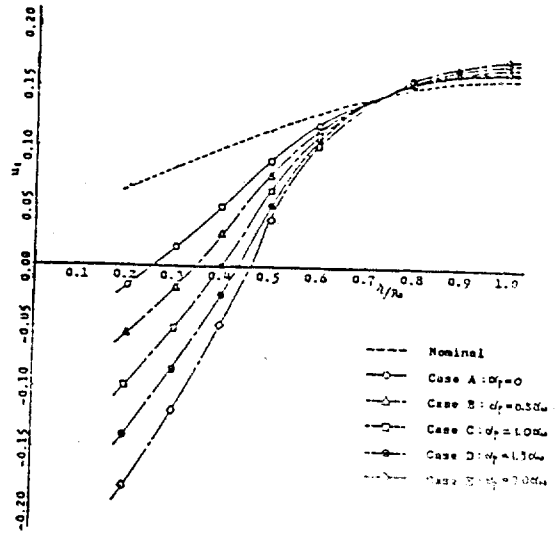

Fig. 9 Harmonic amplitude of axial velocity at propeller plane, $n=1$, Case I-1 (shear)

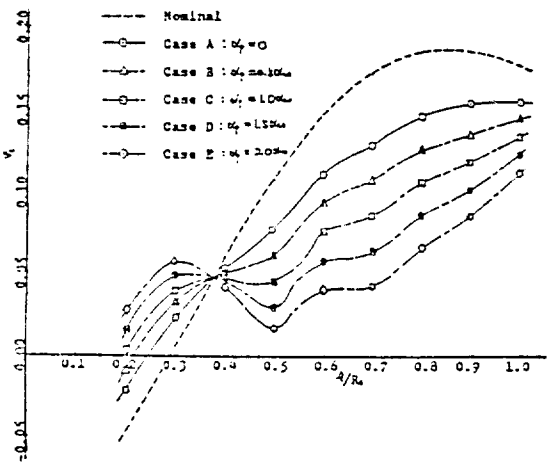

Fig. 10 Harmonic amplitude of tangential velocity at propeller plane, $n=1$, Case I-1 (with shear)

8. Conclusion

From the results we can draw following conclusions,

1) The effects of thickness are very small and they can be ignored.

2) Shear effects are relatively large at inner radii.

3) For equally spaced stator arrays, angular positions of the key blade are not important.

4) Application of blade pitch angles is most effective in changing flow field to reduce non-uniformity.

5) To get effective velocities at the propeller plane, it is recommended to include propeller induced velocities.

References

[1] Young, A.D. and Maas, J.N., Aeronautics Research Council, London, Report and Memorendum No. 1770, 1936.

[2] Von Kármán, T. and Tsien, H.S., "Lifting line theory for a wing in non-uniform flow", Quarterly of Applied Mathmatics, Vol. III, April 1945.

[3] Lighthill, M.J., "The fundamental solution for small steady three-dimensional disturbance to a two-dimensional parallel shear flow", *Journal of Fluid Mechanics*, Vol. 3, November 1957.

[4] Lighthill, M.J., "Contributions to the theory of the Pitot-Tube displacement effect", *Journal of Fluid Mechanics*, Vol. 2, July 1957.

[5] Lighthill, M.J., "Drift", *Journal of Fluid Mechanics*, Vol. 1, January 1956.

[6] Lighthill, M.J., "Corrigenda to Drift", *Journal of Fluid Mechanics*, Vol. 2, May 1957.

[7] Breslin, J.P., "Determination of propeller characteristics in a shear flow", DL Proposal to Office of Naval Research No. P-1650, Davidson Laboratory, November 1976.

[8] Goodman, T.R., "Momentum theory of a propeller in a shear flow", *Journal of Ship Research*, December 1979.

[9] Goodman, T.R. and Valentine, D.T., "Effective inflow velocities into a propeller operating in an axisymmetric shear flow", Stevens Institute of Technology, SIT-DL-80-9-2129, November 1980.

[10] Goodman, T.R. and Breslin, J.P., "Theoretical and experimental induction generated by a propeller in an axially symmetric shear flow", Stevens Institute of Technology, SIT-OE-82-2, February 1982.

[11] Huang, T.T. and Groves, N.C., "Effective wake: Theory and Experiment", 13th ONR Symposium on Naval Hydrodynamics, Tokyo, 1980.

[12] Milne-Thomson, L.M., "Theoretical Hydrodynamics", Third Edition, The Macmillan Company, 1957.

[13] Betz, A., "Aerodynamic theory" Vol. IV, Division J of Applied Airfoil Theory, Peter Smith Publisher, Inc., 1976.

[14] Breslin, J.P., "Ship propeller theory and design", Stevens Institute of Technology, June 1984.

[15] Hadler, J.B. and Cheng, H.M., "Analysis of experimental wake data in way of propeller plane of single and twin-screw ship models", *SNAME Transaction*, Vol. 73, November 1965.